JOURNAL OF BAKU ENGINEERING UNIVERSITY - PHYSICS
2024. Volume 8, Number 2 *Pages 74-80*

UOT: 539.2/.6:539./.04
DOI: https://doi.org/10.30546/09081.2024.102.7065

IMPACT OF SULFUR ION CONCENTRATION ON THE OPTICAL AND STRUCTURAL CHARACTERISTICS OF Ag-Ag_2S Core-Shell NANOSTRUCTURES

Fatma ISMAYILOVA*, Mustafa MURADOV, Mahammad Baghir BAGHIROV, Goncha EYVAZOVA, Sevinj MAMMADYAROVA

Nano Research Laboratory,
Baku State University, Z. Khalilov st.23, AZ-1148,
Baku, Azerbaijan

ARTICLE INFO

Article history:
Received: 2024-11-30
Received in revised form: 2025-01-08
Accepted: 2025-02-10
Available online

Keywords:
Core-shell structures,
Surface Plasmon Resonance,
Ionic diffusion

ABSTRACT

In this study, silver nanoparticles (AgNPs) were synthesized via chemical reduction. Then Ag-Ag_2S core-shell structures were synthesized by simply mixing different concentrations of Na_2S aqueous solution (5,10 and 15mM) and AgNPs. The structural and optical properties of these structures were analyzed. Changes in the structure of the samples were analyzed by X-ray diffraction (XRD). The optical properties and bandgap values were studied using ultraviolet-visible (UV-Vis) spectroscopy. The structural and optical properties of AgNPs revealed clear differences in their physical properties after sulfidation. From the study of optical properties, we determined that Ag-Ag_2S core-shell structures have broadband absorption properties that can be controlled by changing the concentration of sulfur ions in the sulfidation process. Also, because of sulfidation, it was determined that the value of the bandgap of Ag-Ag_2S structures changes.

1. Introduction

In recent years, much attention has been paid to the controlled synthesis of silver-based nanostructures because the catalytic, electronic, and optical properties of these materials can be tuned by changing their composition, shape, size, and structure [1–6]. Among the noble metals, Ag is a promising material for industrial applications because of its non-toxicity and relatively low cost compared to other noble metals. In addition, Ag nanoparticles have a unique localized surface plasmon resonance (SPR) effect that enables light absorption in the visible region of the solar spectrum, thereby enhancing photocatalytic performance [7]. At the same time, Ag nanomaterials are actively used in catalysis, medicine, microelectronics, and other fields due to their surface effect, quantum size effect and high electrical conductivity [8, 9]. As is well known, Ag_2S is a semiconductor with unique physical properties. Ag_2S has low toxicity, non-linear optical properties and exhibits high chemical stability [10-12]. Noble metal-semiconductor hybrid nanostructures are increasingly being explored for their multifunctional capabilities and improved physical and chemical properties compared to their constituents [13, 14]. Among them, Ag-Ag_2S hybrid nanostructures are of practical interest due to their tunable plasmon properties [15]. These optical properties directly depend on the morphology and composition of

the Ag–Ag_2S hybrid nanostructures. Ag-Ag_2S hybrid nanostructures, in particular, exhibit enhanced chemical and thermal stability, tunable plasmonic properties, and exceptional photocatalytic activity. These properties result from synergistic effects between metallic silver and semiconducting silver sulfide components within the nanostructure. These properties of Ag-Ag_2S nanostructures create their highly promising materials for application. These fields can be used in photonic devices, sensor technologies, and biomedical applications [16,17]. At the same time, Ag-Ag_2S nanostructures can be applied as photocatalysts with high efficiency, which allows them to be used in processes such as water splitting and neutralization of natural pollutants [18]. In addition, the wide bandgap of Ag-Ag_2S nanostructures makes them suitable materials for high-quality optical imaging and infrared (IR) detectors. In particular, the use of these materials in applications such as infrared photodetectors and solar cells has become the subject of extensive research [19-21]. Studies on Ag_2S have shown that compared with conventional metal oxide semiconductors, metal sulfides have narrow band gaps and are more efficient in the use of sunlight [22] . Regardless of their morphology, particle size, and coating materials, Ag nanoparticles easily react with sulfides to form silver sulfide (Ag_2S), resulting in Ag-Ag_2S structure and high photocatalytic properties [23].

In this study, the successful synthesis of Ag-Ag_2S core-shell nanostructures was achieved. When Na_2S solution with different concentrations was added to the dispersion of Ag nanoparticles at room temperature, a sulfidation reaction occurred on the surface of Ag nanoparticles and core-shell Ag-Ag_2S structures were formed. The degree of sulfidation of AgNPs can be controlled by changing the concentration of sulfur ions added to the dispersion of AgNPs, which allows the morphological control of Ag-Ag_2S nanostructures. The structural and optical properties of AgNPs and Ag-Ag_2S structures were studied in detail.

2. Materials and methods

2.1 Synthesis of silver nanoparticles and preparation of Ag-Ag_2S core-shell structures

The studied work involved the synthesis of Ag nanoparticles via the chemical reduction method [24,25]. Silver nanoparticles were prepared by reducing silver nitrate using a PVA aqueous solution as a coating agent. A silver nitrate solution was prepared by adding 0.03 g of silver nitrate ($AgNO_3$) to 10 ml of distilled water. Sodium borohydrate ($NaBH_4$) was dissolved in 20 ml of distilled water and added to the PVA solution. The prepared PVA solution was heated to 60°C and stirred. Then $AgNO_3$ solution was added dropwise to the PVA solution. The color of the mixture began to darken with the dropwise addition of $AgNO_3$ solution. After all silver nitrate ($AgNO_3$) solution was added, the mixed solution was stirred in a magnetic stirrer for another 10 min.

Sodium sulfide (Na_2S) was used as a source of sulfur adsorbed on the surface of the synthesized silver nanoparticles. The synthesized Ag-Ag_2S structures were chemically synthesized by changing the concentration of sulfur ions from 5 to 15mM in the Na_2S solution, whereas the concentration of AgNPs remained unchanged. Then, the prepared aqueous solution of sulfur ions was added dropwise to the AgNP solution under continuous stirring. The resultant solution was kept under magnetic stirring for 4 hours and color change of the suspension indicated the formation of Ag-Ag_2S structures. It was washed several times using DI water and the suspension was used for various characterization.

2.2 Analysis methods

The structural investigation was performed utilizing a Rigaku Mini Flex 600 X-ray diffractometer (k 1/4 1.54060 A) using Ni-filtered Cu K_α radiation. Optical properties were examined using the UV-VIS Specord 250 Plus spectrophotometer.

3. Results and discussion

3.1 X-ray diffraction analysis

To determine crystal structure of synthesized AgNPs and Ag-Ag_2S hybrid nanostructures were analyized by XRD and diffractograms are shown in Figure 1. In Figure 1a, peaks corresponding to (111) and (220) planes observed at 2θ=38.33° and 64.63° are characteristic of face-centered cubic crystal structure of AgNPs which revealed JCPDS No. 04-0783 card number [26]. In this pattern observation of broad diffraction peaks indicates that the particle size is small. Figure 1b shows the XRD pattern of Ag-Ag_2S nanostructures synthesized using with 5mM concentration of Na_2S. As can be seen from the pattern, a new peak at 2θ = 32.6° is observed corresponding to (112) index. This peak is characteristic of Ag_2S formed on the surface of AgNPs which is characteristic for monoclinic phase of Ag2S and correspond to (112) Miller index and JCPDS No. 14-0072 card number [27] In the diffraction pattern, by the increasing of the concentration of sulfur ions, the peaks of Ag_2S peaks also increases. This result is due to the increase in the concentration of sulfur ions in the Na_2S solution, which causes AgNPs to be exposed to the more Na_2S solution and more sulfur ions penetrate the nanoparticles. As can be seen from the spectrum in Figure 1b , new peaks for Ag_2S corresponding to the (012), (-112), (-121) and (-103) planes observed at 22.3°, 30.12°, 34.35°, and 37.8°, respectively which correspond to monoclinic phase of Ag_2S. This result is in good agreement with JCPDS No. 14-0072 standard data [28]. This confirms the crystallization of Ag-Ag_2S structures. Thus, an increase in the concentration of Na_2S increases the amount of Ag_2S formed on the surface of the nanoparticles . In addition, although the intensity of the main peak for AgNPs decreased compared with the original sample, the characteristic peaks of AgNPs did not disappear in all spectra, which indicates that not all AgNPs in the sample were converted to Ag_2S and are formed as Ag-Ag_2S heterostructures. The obtained peaks were in good agreement with the characteristic peaks and confirmed the formation of AgNPs and Ag-Ag_2S structures.

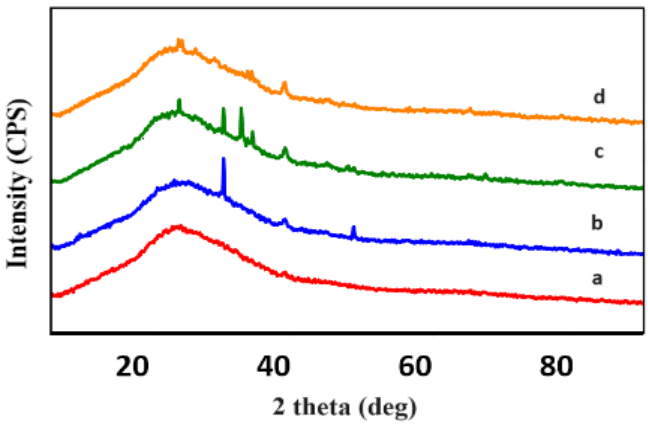

Fig.1 XRD patterns of (a) AgNPs, (b) Ag-Ag_2S (5mM) , (c) Ag-Ag_2S (10mM) , (d) Ag-Ag_2S (15mM)

3.2 UV-Vis spectroscopy

Figure.2A shows the optical absorption spectrum of silver nanoparticles (AgNPs) and Ag-Ag_2S structures with different concentrations. The absorption spectrum shows a characteristic peak at 385 nm. This is consistent with the surface plasmon resonance of AgNPs [29]. This spectrum demonstrates that AgNPs were successfully synthesized. An aqueous solution of Na_2S was added to the dispersion of Ag nanoparticles in different amounts. The sulfidation reaction was monitored by recording the absorption spectra of the reaction solution and altering the Na_2S concentration. However, a decrease in optical absorption was observed after sulfur (S) doping at low concentrations of Na_2S. This decrease is related to AgNP sulfidation and changes in nanoparticle surface properties. When the samples are exposed to the Na_2S solution, the intensity of the peak associated with Ag nanoparticle surface plasmons decreases. Along with the decrease in intensity, a red shift is observed at low and medium concentrations of sulfur ions. This result is due to the effect of Na_2S on the surface of Ag nanoparticles and the reduction of the plasmon oscillations characteristic of Ag nanoparticles. In addition, after the concentration of sulfur ions reached 10 mM, the red shift of the peaks became sharper and an increase in the wavelength of the plasmon peaks of the samples was observed (Figure 2A) . The frequency of plasmon peaks depends on the concentration of free electrons (equation 1) [30]. It is known that a redshift in the wavelength causes decreasing of the frequency. This is due to a decrease in the electron concentration. At the same time, the experimentally observed redshift during the sulfidation process can be attributed to the differences in the sulfidation rate on different sides of the silver nanoparticles [31]. Based on the experimental results, we can conclude that the reduction in the size of the Ag nanoparticle (i.e., the replacement of several atomic layers of the silver nanoparticle with Ag_2S layers) is the most likely explanation for the redshift of AgNPs observed during sulfidation. There are two main reasons why Ag-Ag_2S core-shell structures have broadband absorption properties: First, the red shift of the absorption spectra is associated with the formation of the Ag_2S dielectric layer , which is in good agreement with the literature [33,34]. The reason is that the LSPR (Localized Surface Plasmon Resonance) of Ag nanostructures is sensitive to changes in the surrounding dielectric medium [35]. On the other hand, the broadband absorption of Ag-Ag_2S core-shell structures is related to the gradually changing Ag_2S shell thickness . Using of Na_2S solution, an Ag_2S semiconductor layer is formed on the metallic AgNPs , which is associated with a decrease in electron concentration compared with the first sample.

$$\omega = \sqrt{\frac{ne^2}{\varepsilon_0 m^*}} \qquad (1)$$

ω is the plasmon resonance frequency, n is the concentration of free electrons, e is the elementary charge, ε_0 is the vacuum permeability, and m^* is the effective mass of the electron. According to Equation 1, the calculated concentrations of electrons on the surface of the Ag-Ag_2S structure at different concentrations of Na_2S are given in Table 1. The following is the formation mechanism of Ag-Ag_2S core-shell type structures: sulfidation starts from defects on the surface of Ag nanoparticles [36] and Ag_2S is formed. Sulfur ions undergo two types of diffusion when a small amount of Ag_2S islands are formed on the surface of Ag nanoparticles. It spreads until it reaches its already-formed islands. In the second type of diffusion, with an increase in the concentration of sulfur ions, the amount of Ag_2S on the surface and in the volume relative to Ag increases at different rates. It is clear that surface diffusion is faster than volume diffusion. After penetrating the Ag_2S layers formed by increasing concentrations of sulfur ions, the amount of light reaching

the main surface of Ag decreases, which causes unstable excitation of the plasmon on the Ag surface. At the highest concentration of sulfur ions, the thickness of the surface layers begins to increase. Since the thickness of the volume layer is controlled by diffusion, its thickness does not change. Instead, it further reduced the size of the Ag core.

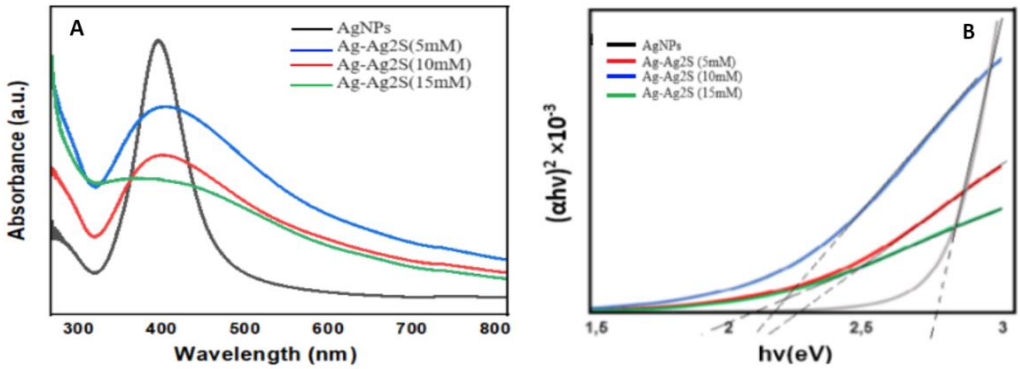

Fig.2 UV-Vis absorption spectra (A) and width of the forbidden band (B) of samples with Ag nanoparticles and Na_2S solution.

Table.1 Plasmonic parameters of Ag-Ag_2S structures prepared at different concentrations.

Nanostructure	**Experimental plasmon peaks (nm)**	**Concentration of plasmon electrons**	**Band gap**
Ag-Ag_2S (5mM)	395	6.92×10^{24} cm $^{-3}$	2.25 eV
Ag-Ag_2S (10mM)	399	6.77×10^{24} cm $^{-3}$	2.19 eV
Ag-Ag_2S (15mM)	403	$6.1\,5\times10^{24}$ cm $^{-3}$	2.10 eV

The band gap values of the samples were determined using the Tauc method.

$$(\alpha h\nu)^2 = A(h\nu - E_g) \qquad (2)$$

$h\nu$ is the photon energy, A is a constant that depends on the structure and type of the sample, E_g is the band gap, and the value of n depends on the nature of the transition: n = 2 for direct allowed transition, n=1/2 for indirect allowed transition, α is the absorption coefficient, its value is obtained from the Beer-Lambert formula. As shown in Figure 2B , the pure AgNPs have a band gap of 2.8 eV. This value is related to the optical properties of Ag and quantum size effects. Also, as seen in Figure 2B, the bandgap at different concentrations of Na_2S solution obtained different values: 2.25 eV at 5 mM concentration, 2.19 eV at 10 mM concentration, and 2.10 eV at 15 mM concentration. When Ag nanoparticles react with Na_2S solution, Ag_2S is formed on their surface. The kinetics of this reaction depend on the solution concentration. At higher concentrations, the reaction was faster, resulting in more Ag_2S being formed. The thickness of the Ag_2S layer formed on the surface of Ag particles during the reaction increased with increasing concentration. In 5 mM Na_2S solution, the surface of Ag particles was covered with a small amount of Ag_2S, as a result, the band gap decreased to 2.25 eV. In 10 mM and 15 mM Na_2S solutions, the Ag_2S layer is thicker, and as a result, the bandgap decreases from 2.19 eV to 2.10 eV, respectively. The formation of Ag_2S narrows the band gap of Ag nanoparticles because the Ag_2S material has a different electronic structure than pure Ag. As the Ag_2S layer on the surface thickens, the quantum size effect of the Ag nanoparticle weakens and the band gap decreases. According to the available literature, the bandgap of Ag_2S nanocrystals is in the range of E_g = 0.9-1.1 eV [37]. Consequently, the analysis of the results shows that the introduction of sulfur (S) can

lead to changes in the bandgap of Ag-Ag_2S core-shell type structures. The reason for this is that the excited electrons passing into the conduction band of Ag_2S easily transfer to silver at the Ag–Ag_2S interface. The formation of Ag and Ag_2S heterostructure changes the structure of the band gap of Ag_2S at the interface, facilitates the separation of charges, and reduces the recombination of charge carriers.

4. Conclusion

In this study, silver nanoparticles were synthesized via chemical reduction. Then, Ag-Ag_2S core-shell structures were prepared by adding different concentrations of Na_2S solution to AgNPs . The properties of AgNPs and Ag-Ag_2S structures were studied. The structural analysis results showed that a layer of Ag_2S formed on the surface of the AgNPs because of the sulfidation process. In addition, there was a decrease in the degree of crystallization of AgNPs. This structural change depends on the increase in the concentration of sulfur ions. Moreover, UV-Vis spectroscopy showed that the intensity of the plasmon oscillation peaks of the silver nanoparticles decreased and a red shift occured with increasing concentrations. In addition, the band gap decreased from 2.25 eV to 2.10 eV. It can be associated with the formation of Ag_2S nanoparticles .

REFERENCES

1. B.S.Hoener et al. Plasmonic sensing and control of single-nanoparticle electrochemistry, Chem 4 (**2018**) 1560-1585.
2. S.Rostami, A.Mehdinia, A.Jabbari. Seed-mediated grown silver nanoparticles as a colorimetric sensor for detection of ascorbic acid, Spectrochimica Acta Part A Molecular and Biomolecular Spectroscopy, 180 (**2017**) 204-210.
3. M.Chen, Y.He, J.Zhu. Preparation of Au–Ag bimetallic nanoparticles for enhanced solar photothermal conversion, International Journal of Heat and Mass Transfer, 114 (**2017**) 1098- 1104.
4. A.Decharat, S.Wagle, S.Jacobsen, F.Melandso. Using Silver Nano-Particle Ink in Electrode Fabrication of High Frequency Copolymer Ultrasonic Transducers: Modeling and Experimental Investigation. Sensors, 15 (**2015**) 9210–9227.
5. Q.Huang, W.Shen, Q.Xu, R.Tan, W.Song. Properties of polyacrylic acid-coated silver nanoparticle ink for inkjet printing conductive tracks on paper with high conductivity. Mater. Chem. Phys, 147 (**2014**) 550–556.
6. A.Hu, J.Y.Guo, H.Alarifi, G.Patane, Y.Zhou, G.Compagnini, C.X.Xu. Low temperature sintering of Ag nanoparticles for flexible electronics packaging. Appl. Phys. Lett, 97 (**2010**) 153117.
7. J.Low et al. Direct evidence and enhancement of surface plasmon resonance effect on Ag-loaded TiO_2 nanotube arrays for photocatalytic CO_2 reduction. Applied Surface Science, 434 (**2018**) 423-432 .
8. P.Panchal, D.R.Paul, A.Sharma, P.Choudhary, P.Meena, S.P.Nehra. Biogenic mediated Ag/ZnO nanocomposites for photocatalytic and antibacterial activities towards disinfection of water, J.Colloid Sci, 563 (**2020**) 370–380.
9. X.Liu, J.Iocozzia, Y.Wang, X.Cui, Y.Chen, S.Zhao, Z.Lee, Z.Lin. Noble metal-metal oxide nanohybrids with tailored nanostructures for efficient solar energy conversion, photocatalysis and environmental remediation. Energy Environ. Sci, 10 (**2017**) 402–434.
10. J.Feng, X.Li, Z.Shi, C.Zheng, X.Li, D.Leng, Y.Wang, J.Liu, L.Zhu. Adv. Opt. Mater , 8 (**2020**) 1901762.
11. C.Ding, Y.Huang, Z.Shen, X.Chen. Adv. Mater , 33 (**2021**) 2007768.
12. A.Badawi, S.S.Alharthi. Mater. Sci. Semicond. Process, 116 (**2020**) 105139.
13. N.Zhang et al. Function-oriented engineering of metal-based nanohybrids for photoredox catalysis: exerting plasmonic effect and beyond, Chem, 4.8 (**2018**) 1832–1861.
14. S.I.Sadovnikov et al. Enhanced photocatalytic hydrogen evolution from aqueous solutions on Ag_2S/Ag heteronanostructure, International Journal of Hydrogen Energy, 42 (**2017**) 25258-25266.
15. J.Zhao, Hundred, J.Xing, Y.Zou, H.Liu, H.Zhang, W.Yu, H.Idriss, C.Guo. Effect of Ag_2S Nanocrystals/Reduced Graphene Oxide Interface on Hydrogen Evolution Reaction. Catalysts, 10 (**2020**) 948.

16. J.Xiong, C.Han, W.Li, Q.Sun, J.Chen, S.Chou, Z.Li, S.Dou. Ambient synthesis of a multifunctional 1D/2D hierarchical Ag-Ag_2S nanowire/nanosheet heterostructure with diverse applications. CrystEngComm, 18 (**2016**) 930-937.
17. M.M.Shahjamali, Y.Zhou, N.Zaraee, C.Xue, J.Wu, N.Large, C.A.Mirkin. Ag–Ag_2S hybrid nanoprisms: structural versus plasmonic evolution, Acs Nano, 10 (**2016**) 5362-5373.
18. B.Díez-Buitrago et al. Facile synthesis and characterization of Ag/Ag_2S nanoparticles enzymatically grown in situ and their application to the colorimetric detection of glucose oxidase,ChemistrySelect, 4.28 (**2019**) 8212-8219.
19. A.Pradyasti et al. Ag–Ag_2S hybrid nanoplates with unique heterostructures: Facile synthesis and photocatalytic application, Journal of Alloys and Compounds, 826 (**2020**) 154191.
20. X.H.Wang, B.Shi, Y.Fang, F.Rong, F.F.Huang, R.H.Que, M.W.Shao. High capacitance and rate capability of a Ni_3S_2 @CdS core-shell nanostructure supercapacitor, J. Mater. Chem. A, 5 (**2017**) 7165-7172.
21. R.Marin et al. Nanoprobes for Biomedical Imaging with Tunable Near-Infrared Optical Properties Obtained via Green Synthesis, Advanced Photonics Research, 3.1 (**2022**) 2100260.
22. D.Ruiz et al. Ag/Ag_2S nanocrystals for high sensitivity near-infrared luminescence nanothermometry, Advanced Functional Materials, 27.6 (**2017**) 1604629.
23. B.M.Al-Shehri, M.Shkir, T.M.Bawazeer, S.AlFaify, M.S.Hamdy. Phys. E, 121 (**2020**) 114060.
24. S.H.Lee, B.H.Jun. Silver Nanoparticles: Synthesis and Application for Nanomedicine, Int. J. Mol.Sci, 20 (**2019**) 865.
25. A.Syafiuddin, Salmiati, M.R.Salim, A.B.H.Kueh, T.Hadibarata, H.A.Nur. Review of silver nanoparticles: Research trends, global consumption, synthesis, properties, and future challenges. J. Clin. Chem. Soc, 64 (**2017**) 732–756.
26. J.Lu, D.Liu, J.Dai. J. Mater. Sci.: Mater. Electron, 30 (**2019**) 15786–15794.
27. K.Sahraoui, N.Benramdane, M.Khadraoui, R.Miloua, C.Mathieu. Characterization of silver sulphide thin films prepared by spray pyrolysis using a new precursor silver chloride, Sensors & Transducers, 27 (**2014**) 319-325.
28. A.Gusev, S.J.S.Sadovnikov. Acanthite–argentite transformation in nanocrystalline silver sulfide and the Ag_2S/Ag nanoheterostructure, Semiconductors, 50 (**2016**) 682–687.
29. K.Khurana, N.Jaggi. Localized surface plasmonic properties of Au and Ag nanoparticles for sensors: A review, Plasmonics, 16.4 (**2021**) 981-999.
30. M.B.Gebeyehu, T.F.Chala, S.Y.Chang, C.M.Wu, J.Y.Lee. RSC Adv, 7 (26) (**2017**) 16139–16148.
31. M.M.Shahjamali et al. Ag–Ag_2S hybrid nanoprisms: structural versus plasmonic evolution, Acs Nano, 10.5 (**2016**) 5362-5373.
32. J.Xiong et al. Ambient synthesis of a multifunctional 1D/2D hierarchical Ag–Ag_2S nanowire/nanosheet heterostructure with diverse applications, CrystEngComm, 18 (**2016**) 930–937.
33. J.Zeng, J.Tao, D.Su, Y.Zhu, D.Qin. Selective sulfuration at the corner sites of a silver nanocrystal and its use in stabilization of the shape, Nano Lett, 11 (**2011**) 3010–3015.
34. M.Pang, J.Hu, H.C.Zeng. Synthesis, morphological control, and antibacterial properties of hollow/solid Ag_2S/Ag heterodimers, Journal of the American Chemical Society, 132.31 (**2010**) 10771-10785.
35. G.Park,C.Lee, D.Seo, H.Song. Full-Color Tuning of Surface Plasmon Resonance by Compositional Variation of Au@Ag Core-Shell Nanocubes with Sulfides, Langmuir, 28 (**2012**) 9003–9009.
36. R.Zamiri, H.A.Abbastabar, A.Zakaria, G.Zamiri, M.Shabani, B.Singh, J.M.F.Ferreira. Chem.cent. J, 9 (**2015**) 1–6.
37. A.Nekooei, M.R.Miroliaei, M.S.Nejad, & H.Sheibani, Enhanced visible-light photocatalytic activity of ZnS/S-graphene quantum dots reinforced with Ag_2S nanoparticles. *Materials Science and Engineering: B*, 284, (**2022**). 115884.